

5-1-1995

Evidence of dilution-induced Griffiths instabilities in $K_2Cu_{1-x}Zn_xF_4$ and $Fe_{1-x}Zn_xF_2$

Christian Binek

University of Nebraska-Lincoln, cbinek@unl.edu

Wolfgang Kleeman

Angewandte Physik, Gerhard-Mercator Universitat-Gesamthochschule-Duisburg, Federal Republic of Germany,
wolfgang.kleemann@uni-due.de

Follow this and additional works at: <http://digitalcommons.unl.edu/physicsbinek>



Part of the [Physics Commons](#)

Binek, Christian and Kleeman, Wolfgang, "Evidence of dilution-induced Griffiths instabilities in $K_2Cu_{1-x}Zn_xF_4$ and $Fe_{1-x}Zn_xF_2$ " (1995). *Christian Binek Publications*. 5.

<http://digitalcommons.unl.edu/physicsbinek/5>

This Article is brought to you for free and open access by the Research Papers in Physics and Astronomy at DigitalCommons@University of Nebraska - Lincoln. It has been accepted for inclusion in Christian Binek Publications by an authorized administrator of DigitalCommons@University of Nebraska - Lincoln.

Evidence of dilution-induced Griffiths instabilities in $K_2Cu_{1-x}Zn_xF_4$ and $Fe_{1-x}Zn_xF_2$

Ch. Binek and W. Kleemann

Angewandte Physik, Gerhard-Mercator-Universität-Gesamthochschule-Duisburg, D-47048 Duisburg, Federal Republic of Germany

(Received 20 January 1995; revised manuscript received 27 February 1995)

Weak quasistatic singularities are evidenced within the Griffiths regime of temperatures $T_c(x) \leq T \leq T_c(x=0)$ in the diluted antiferromagnet $Fe_{1-x}Zn_xF_2$, $x=0.53$, and in the diluted ferromagnet $K_2Cu_{1-x}Zn_xF_4$, $x=0.2$, by measurements of the magnetic susceptibility, χ' vs T , in zero external field. Significant deviations from classical ($\gamma=1$, for $Fe_{0.47}Zn_{0.53}F_2$) and nonclassical ($\gamma>1$, for $K_2Cu_{0.8}Zn_{0.2}F_4$) Curie-Weiss-type behavior, $\chi' \propto [T - T_c(x)]^{-\gamma}$, are found just below $T_c(x=0)$ by using linear-regression data analysis.

Since Griffiths' rigorous theoretical investigation of the diluted Ising ferromagnet¹ it is known that its magnetization is a nonanalytic function of the magnetic field H at $H=0$ for all temperatures $T < T_G$. The Griffiths temperature T_G is defined as the critical temperature $T_c(x=0)$ of the undiluted system. If $1-x$, the concentration of magnetic ions, exceeds the percolation threshold, a global phase transition sets in at $T_c(x) > 0$, which is accompanied by strong singularities of the free energy. In that case, the Griffiths phase exists within $T_c(x) \leq T \leq T_G$. It is characterized by the existence of weak singularities of the free energy. A physically motivated picture of the Griffiths phase is given by the assumption of a continuous series of local phase transitions within $T_c(x) \leq T \leq T_G$. Arbitrarily large pure and differently diluted clusters are at the origin of this local quasicritical behavior. They must occur in the thermodynamic limit of infinite sample volume.

However, experimental evidence for the Griffiths anomalies is not easy to find. Recent theoretical²⁻⁴ and Monte Carlo studies⁵ mainly focused on the dynamical signature of the Griffiths phase. They predict a nonexponential tail of the temporal decay of the spin autocorrelation function. This contrasts with the simple exponential relaxation of magnetization in a usual paramagnet. In fact, an experimental hint at a dynamical signature of the Griffiths phase was derived from inelastic neutron-scattering data on the diluted Heisenberg antiferromagnet $KMn_{0.3}Ni_{0.7}F_3$.⁶ However, the results are far from being totally convincing.

Much clearer evidence was recently obtained on a field-induced Griffiths phase of the metamagnetic compounds $FeCl_2$ (Ref. 7) and $FeBr_2$ (Ref. 8) by measurements of the complex susceptibility in the presence of an axial external magnetic field. The analogy with the conventional¹ Griffiths system consists in the fact that both dilution and external field suppress the respective order parameters. However, the nature of the corresponding fluctuations, which are crucial prerequisites for the Griffiths instabilities, are fundamentally different. They are static in the diluted system, but dynamic, viz., induced by fluctuating demagnetizing fields, in the antiferromagnet exposed to an external field. There is, hence, no one-to-one mapping from the field-induced to the dilution-induced Griffiths phase.

It is a principal problem of any experimental investigation of the dilution-induced Griffiths phase to make sure, that

anomalies, if any, are not due to crystalline imperfections like concentration gradients, but originate from the natural statistics of the cluster distribution which accompanies the perfect crystal growth. That is why we used crystals of extremely high quality. On the one hand, we studied a sample of the antiferromagnetic solid solution $Fe_{0.47}Zn_{0.53}F_2$, the batch of which was described as a crystal of extremely high homogeneity.⁹ Our sample has extensively been used for studies of the critical behavior, which require extremely small concentration gradients in order to avoid artificial rounding of the phase transition.¹⁰ The other system is the ferromagnetic solid solution, $K_2Cu_{0.8}Zn_{0.2}F_4$, the batch of which was shown to yield very homogeneous samples.¹¹ Its quasi-two-dimensional (2D) magnetic behavior offers the additional advantage of revealing particularly strong spin fluctuations when compared with conventional 3D systems.

A superconducting quantum interference device (SQUID) magnetometer (Quantum Design MPMS 5S) was used to measure the temperature dependence of the complex parallel magnetic susceptibility in zero magnetic field at frequencies $f=10$ Hz on $Fe_{0.47}Zn_{0.53}F_2$ and $f=7$ and 300 Hz on $K_2Cu_{0.8}Zn_{0.2}F_4$. On $Fe_{0.47}Zn_{0.53}F_2$ one has to detect the magnetization response parallel to the tetragonal c axis, whereas for $K_2Cu_{0.8}Zn_{0.2}F_4$ the easy axis is perpendicular to the c axis. Neglecting the small intraplanar magnetic anisotropy¹² one can choose an arbitrary axis within the c plane. We focused our attention on the paramagnetic tail of the χ' vs T curves at $T > T_c(x)$. Virtually no losses, $\chi'' < 10^{-4}\chi'$, are observed in this temperature range. In the case of $Fe_{0.47}Zn_{0.53}F_2$ [$T_c(x)=36.7$ K] we measured the susceptibility within $40 \leq T \leq 170$ K at constant temperature steps of $\Delta T=0.1$ K. The result is shown in the inset of Fig. 1 (curve 1). No deviations from conventional paramagnetic behavior are visible unless further analysis is done as described below.

For temperatures $T > T_N(x=0) = 78.3$ K (Ref. 13) one expects that χ' vs T obeys a simple Curie-Weiss law,

$$\chi' = C/(T - \Theta), \quad (1)$$

where C is a frequency-dependent proportionality constant and $\Theta < 0$ the global Curie temperature of the antiferromagnet. From a theoretical point of view,¹⁴ Eq. (1) is an approximation assuming the temperature-independent background χ'_0 to be much smaller than $\chi'(T \approx T_N)$. Experimentally, Eq. (1) holds for pure FeF_2 at $T/T_N(x=0) > 1$,¹⁴ and is expected

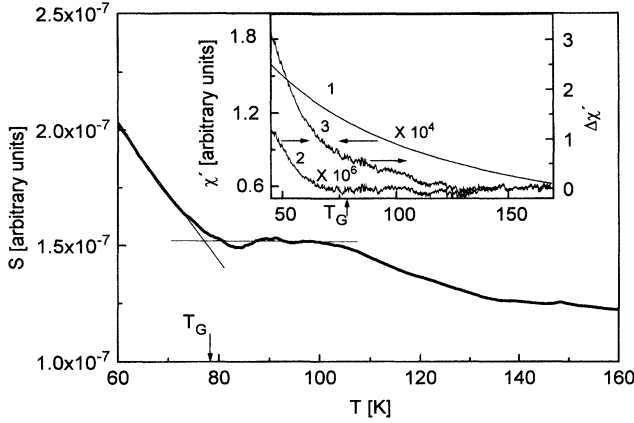


FIG. 1. S vs T (see text) derived from linear regression analysis of χ' vs T data (inset, curve 1) of $\text{Fe}_{0.47}\text{Zn}_{0.53}\text{F}_2$ at constant frequency $f=10$ Hz. The Griffiths temperature $T_G=78.3$ K is indicated by arrows. The linearized S vs T data (straight lines) within $60 \leq T \leq 75$ K and $85 \leq T \leq 100$ K, respectively, intersect at $T=77.1$ K. The inset (curves 2 and 3) shows deviations $\Delta\chi'$ from Eq. (1) which arise from direct subtraction of best-fit curves from the χ' vs T data for fitting intervals $T_0 \leq T \leq T_1$ with $T_1=170$ K and $T_0=80$ (curve 2) and 120 K (curve 3), respectively.

to apply also to $\text{Fe}_{0.47}\text{Zn}_{0.53}\text{F}_2$. Taking into account $T_N(x=0.53)=36.7$ K (Ref. 10) the Curie-Weiss law should be applicable at least down to $T \geq 50$ K. However, within the Griffiths phase, we expect quasicritical contributions to χ' vs T . They arise from magnetic clusters, which undergo local phase transitions at transition temperatures $T_N(x) \leq T_N \leq T_N(x=0)$. Hence, one expects a significant deviation of the χ' vs T data from the temperature dependence given by Eq. (1). It should set in just below the Griffiths temperature $T_G=T_N(x=0)$ and is expected to increase with decreasing temperature owing to the increasing number of clusters which already underwent a local phase transition on cooling. Unfortunately, it appears impossible to verify directly the expected deviations from Eq. (1) by simply subtracting a best-fitted model curve from the measured data. On one hand, if the fitting interval contains the expected Griffiths temperature, e.g., $50 \leq T \leq 100$ K, an equipartition of very small errors is found throughout this interval because of the *a priori* compromise mediating between data at $T > T_G$ and $T < T_G$. On the other hand, for fitting intervals $T_0 \leq T \leq T_1$ with $T_0 > T_G$ we always find severe deviations, $\Delta\chi'$, at the lower bound, $T < T_0$. This is shown for $T_1=170$ K, and $T_0=80$ (curve 2) and 120 K (curve 3), respectively. Obviously, these errors are systematically due to deviations from the mean-field equation (1) when approaching $T_N(x)$ rather than to the onset of Griffiths-type instabilities. A more sophisticated linear regression analysis is therefore in order. To this end we rearrange Eq. (1) for a linear regression analysis, $1/\chi' = T/C - \Theta/C$, and introduce the sum

$$D_{j,n} = \sum_{i=j}^{j+n} [1/\chi'_i(T_i) - T_i/C + \Theta/C]^2 \quad (2)$$

with (χ'_i, T_i) , the i th point of the χ' vs T data set. $D_{j,n}$ measures the deviation of the χ' vs T data from their de-

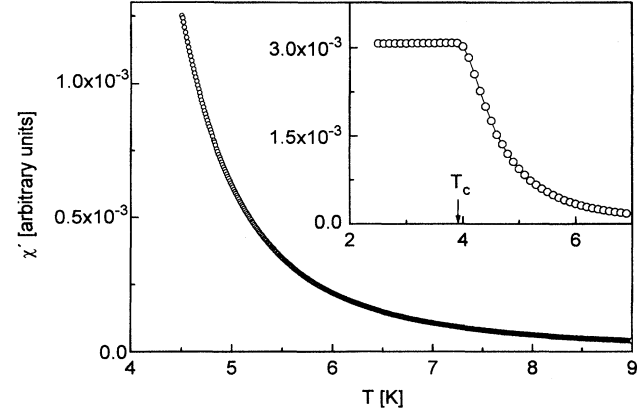


FIG. 2. χ' vs T for $\text{K}_2\text{Cu}_{0.8}\text{Zn}_{0.2}\text{F}_4$ at frequency $f=300$ Hz corrected for demagnetization. The demagnetizing factor is obtained from the reciprocal saturation value of the original χ' vs T curve at $f=7$ Hz (inset) for $T < T_c=3.9$ K.

scription by Eq. (1) in the temperature interval $T_j \leq T_i \leq T_{j+n}$. The minimization of $D_{j,n}$ with respect to $1/C$ and Θ/C gives simple analytic expressions for the parameters C and Θ within the framework of linear regression analysis. Once the best values C and Θ are found one can compute the quantity

$$S_j = \left[(n-1)^{-1} \sum_{i=j}^{j+n} [\chi'_i(T_i) - C/(T_i - \Theta)]^2 \right]^{1/2}$$

as a measure of the quality of the theoretical description of the data.

Figure 1 shows the most interesting part of the computed S_1 vs T_{1+n} curve (S vs T , for short) starting at $T_{200}=60$ K up to $T_{1200}=160$ K. Obviously the width of the regression interval is continuously increasing from the Griffiths region into the paramagnetic region. That is why even in the absence of any Griffiths-type anomaly one would expect S vs T to decrease with increasing temperature. This is simply due to the fact that Eq. (1) describes the asymptotic high- T regime, but starts to fail when approaching $T_N(x)$. However, in addition to this, S vs T shows a significant change of slope at $T=77.1$ K obtained from the intersection of extrapolated parts of S vs T linearized within $60 \leq T \leq 75$ K and $85 \leq T \leq 100$ K, respectively. This temperature nearly coincides with the Griffiths temperature $T_G=78.3$ K. The gradual change of slope within $75 \leq T \leq 85$ K is primarily due to the gradual dying-out of Griffiths-type critical clusters as $T \rightarrow T_G$. In addition, the influence of the “noise-free” regime at $T > T_G$ on the global noise figure, S_1 , grows in proportion to $T - T_G$.

A similar analysis is made for the χ' vs T data of the ferromagnetic $\text{K}_2\text{Cu}_{1-x}\text{Zn}_x\text{F}_4$ [$x=0.2$, $T_c(x)=3.90$ K]. Figure 2 shows the χ' vs T data within $4.5 \leq T \leq 9$ K at temperature steps $\Delta T=0.01$ K after correction for demagnetization.¹⁵ The demagnetization factor was determined from the inverse of the constant saturation value of the uncorrected χ' vs T data below the global phase transition temperature $T_c(x)$. As can be seen from the data in Fig.

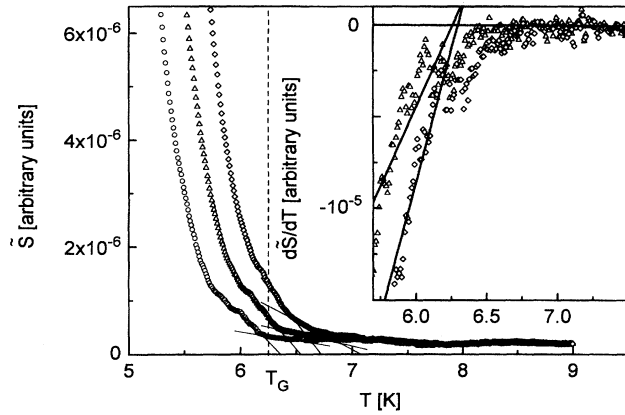


FIG. 3. \bar{S} vs T (see text) derived from linear regression analysis of χ' vs T data of $\text{K}_2\text{Cu}_{0.8}\text{Zn}_{0.2}\text{F}_4$ (Fig. 2) for different widths of the regression interval $\delta T = 0.4$ (circles), 0.5 (triangles), and 0.6 K (diamonds), respectively. The Griffiths temperature $T_G = 6.25$ K is indicated by a vertical dashed line. The linearized \bar{S} vs T data (straight lines) within temperature intervals $\Delta T = 0.2$ K below and above the respective bending points intersect close to T_G . The inset shows the derivatives $d\bar{S}/dT$ vs T for $\delta T = 0.5$ (triangles) and 0.6 K (diamonds), whose linear extrapolations (straight lines) vanish at $T = 6.24$ and 6.29 K, respectively.

2 (inset), rounding of the transition occurs within an interval of less than $\Delta T \approx 0.05$ K, i.e., $|T/T_c - 1| < 10^{-2}$. It is, hence, nearly as sharp as the transition of the pure compound K_2CuF_4 .¹¹

In contrast to $\text{Fe}_{1-x}\text{Zn}_x\text{F}_2$, even pure K_2CuF_4 shows deviations from mean-field behavior, Eq. (1), throughout the paramagnetic phase. An adequate description is given by¹⁵

$$\chi' = C(T - T_c)^{-\gamma}, \quad (3)$$

where the critical exponent varies between $\gamma \approx 1$ close to $T_c = 6.25$ K (Ref. 12) and $\gamma \approx 2$ for $T \approx 2T_c$. This behavior is explained¹⁵ by a series of crossovers from 2D Heisenberg to 2D xy , 3D xy and, eventually, dipolar critical behavior. A similar behavior might also be expected for the diluted system. Again, a direct subtraction of best-fit curves, Eq. (3), from the measured data does not prove the Griffiths conjecture because of the ambiguities outlined above. Therefore, similarly as in the case of $\text{Fe}_{1-x}\text{Zn}_x\text{F}_2$ we prefer a linear regression analysis starting from the logarithmic form of Eq. (3), $\ln \chi' = \ln C - \gamma \ln(T - T_c)$, where $T_c = 3.9$ K. In a manner analogous to Eq. (2) we introduce the quantities

$$\bar{D}_{j,n} = \sum_{i=j}^{j+n} [\ln \chi'_i(T_i) - \ln C + \gamma \ln(T_i - T_c)]^2 \quad (4)$$

and

$$\bar{S}_j = \left[(n-1)^{-1} \sum_{i=j}^{j+n} [\chi'_i(T_i) - C(T_i - T_c)^{-\gamma}]^2 \right]^{1/2}.$$

Figure 3 shows \bar{S}_j vs T_{j+n} (\bar{S} vs T , for short). Here \bar{S} results from the linear regression procedure within the continuously shifted temperature interval $T_j \leq T_i \leq T_{j+n}$ of size

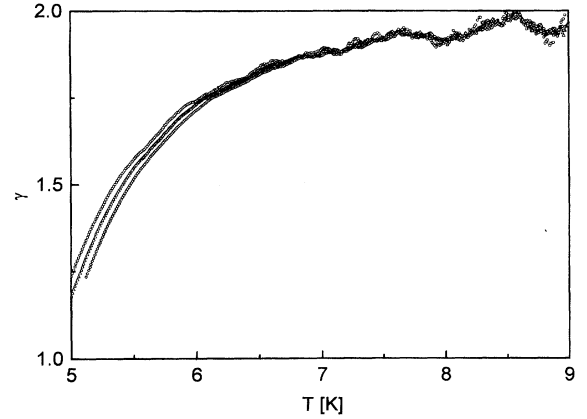


FIG. 4. γ vs T derived from linear regression analysis (see text) of χ' vs T of $\text{K}_2\text{Cu}_{0.8}\text{Zn}_{0.2}\text{F}_4$ (Fig. 2) for regression intervals $\delta T = 0.4$ (circles), 0.5 (triangles), and 0.6 K (diamonds).

$\delta T = n\Delta T$. It is plotted as a function of the upper boundary T_{j+n} . This procedure has been done for $\delta T = 0.4, 0.5,$ and 0.6 K, hence, $n = 40, 50,$ and 60 , respectively. At variance with the analysis applied to $\text{Fe}_{1-x}\text{Zn}_x\text{F}_2$ this is possible owing to the very high temperature resolution ($\Delta T = 0.01$ K). Enhanced sensitivity to the onset of the Griffiths regime may be anticipated. This is indeed the case. Whereas we observe a nearly constant very low level value of $\bar{S} \approx 2 \times 10^{-7}$ above $T_G = 6.25$ K, there is a steep increase of \bar{S} just below T_G owing to Griffiths-type anomalies. It is seen that the change of slope $d\bar{S}/dT$ is sharpest for $\delta T = 0.4$ K. It becomes more smeared and shifted to higher temperatures as δT increases to 0.5 and 0.6 K, respectively. This is easily understood when considering that the influence of “noisy” data originating from $T < T_G$ to \bar{S} at $T > T_G$ increases with increasing width of the interval δT . In fact, the intersection temperatures of linear extrapolations of steep and flat portions (widths: 0.2 K) of \bar{S} vs T below and above the respective bending points reveal $T_G = 6.20, 6.35,$ and 6.47 K, respectively (Fig. 3), for $\delta T = 0.4, 0.5,$ and 0.6 K. Obviously, the $\delta T = 0.4$ value, $T_G = 6.20$ K, lies closest to the expected value. As an alternative way to obtain T_G without being puzzled by smearing effects around T_G we propose a linear extrapolation of the slope $d\bar{S}/dT$ which is expected to vanish at T_G . As shown in the inset of Fig. 3, we find $T_G = 6.24$ and 6.29 K, respectively, from the $\delta T = 0.5$ and 0.6 K data sets.

Figure 4 shows the γ values which are derived from the regression analysis of the susceptibility. Similarly as observed on K_2CuF_4 ,¹⁵ γ shows a strong temperature dependence. It decreases from $\gamma \approx 2$ at $T \approx 2T_c$ to $\gamma \approx 1.2$ at $T \approx 1.2T_c$. Significant influence of randomness (random-exchange critical behavior) is not evident. We rather find a slight dependence on the width of the regression interval. It is remarkable that the splitting of the curves sets in at a temperature close to T_G and increases smoothly with decreasing temperature. Very probably this is due to the strong T dependence of γ at $T \leq T_G$. Concavity of $\ln \chi'$ vs $\ln(T - T_c)$ yields decreasing slopes, $\gamma = -\Delta \ln \chi' / \Delta \ln(T - T_c)$ as δT increases.

In conclusion, strong evidence for dilution-induced Griffiths anomalies has been revealed by the temperature depen-

dence of the parallel ac susceptibility of the 3D antiferromagnetic Ising system $\text{Fe}_{1-x}\text{Zn}_x\text{F}_2$ and the 2D ferromagnetic Heisenberg system $\text{K}_2\text{Cu}_{1-x}\text{Zn}_x\text{F}_4$, respectively. Instead of very low relaxation-time experiments suggested by recent theory²⁻⁴ we performed quasistatic, very-low-frequency susceptibility measurements taking advantage of highly sensitive SQUID susceptometry. At $T < T_G$ weak singularities are superimposed to the global mean field ($\text{Fe}_{1-x}\text{Zn}_x\text{F}_2$) or quasiscritical ($\text{K}_2\text{Cu}_{1-x}\text{Zn}_x\text{F}_4$) susceptibility signal without visibly changing its analytical shape. They merely give rise to enhanced noise when performing linear regression analysis without changing the Curie-Weiss-type model functions. Unfortunately, we are not aware of adequately modified model functions, which account for the weak singularities and,

hence, would yield optimal fits in the Griffiths regime. Obviously theoretical expressions of the static response function in the Griffiths regime are needed. A heuristic description should be possible by using the finite-size limited local criticality of the susceptibility and appropriate cluster distribution functions as in the case of the field-induced Griffiths phase.¹⁶ More theoretical research in this field is clearly desirable.

Thanks are due to I. Yamada and to V. Jaccarino for providing excellent samples of $\text{K}_2\text{Cu}_{0.8}\text{Zn}_{0.2}\text{F}_4$ and $\text{Fe}_{0.47}\text{Zn}_{0.53}\text{F}_2$, respectively. This work was supported by Deutsche Forschungsgemeinschaft through Sonderforschungsbereich 166.

¹R. B. Griffiths, *Phys. Rev. Lett.* **23**, 17 (1969).

²M. Randeria, J. P. Sethna, and R. G. Palmer, *Phys. Rev. Lett.* **54**, 1321 (1985).

³D. Dahr, M. Randeria, and J. P. Sethna, *Europhys. Lett.* **5**, 485 (1988).

⁴A. J. Bray, *Phys. Rev. Lett.* **60**, 720 (1988).

⁵V. B. Andreichenko, W. Selke, and A. L. Talapov, *J. Phys. A* **25**, 283 (1992).

⁶R. G. Lloyd and P. W. Mitchell, *J. Phys. C* **1**, 5013 (1989).

⁷Ch. Binek and W. Kleemann, *Phys. Rev. Lett.* **72**, 1287 (1994).

⁸Ch. Binek, M. M. P. de Azevedo, W. Kleemann, and D. Bertrand, *J. Magn. Magn. Mater.* **140-144**, 1555 (1995).

⁹D. P. Belanger, A. R. King, J. B. Ferreira, and V. Jaccarino, *Phys. Rev. B* **37**, 226 (1988).

¹⁰P. Pollak, W. Kleemann, and D. P. Belanger, *Phys. Rev. B* **38**, 4773 (1988).

¹¹Y. Okuda, Y. Tohi, and I. Yamada, *J. Phys. Soc. Jpn.* **49**, 936 (1980).

¹²H. Yamazaki, Y. Morishige, and M. Chikamatsu, *J. Phys. Soc. Jpn.* **50**, 2872 (1981).

¹³Y. Shapira, *Phys. Rev. B* **2**, 2725 (1970).

¹⁴M. E. Lines, *Phys. Rev.* **156**, 543 (1967).

¹⁵A. Dupas and J. P. Renard, *J. Phys. C* **1**, 213 (1976).

¹⁶Ch. Binek and W. Kleemann, *Acta Phys. Slovaca* **44**, 435 (1994).